Int J Coal Sci Technol (2015) 2(4):325–332
DOI 10.1007/s40789-015-0091-0

Orthogonal experiment design of EMI of security monitoring system in coal mines

Xiang Liu[1] · Chaoqun Jiao[1] · Aifen Yao[1]

Received: 15 June 2015 / Revised: 22 October 2015 / Accepted: 23 October 2015 / Published online: 24 November 2015

Abstract Security monitoring system of coal mines is indispensable to ensure the safe and efficient production of colliery. Due to the special and narrow underground field of the coal mine, the electromagnetic interference can cause a series of misstatements and false positives on the monitoring system, which will severely hamper the safe production of coal industry. In this paper, first, the frequency characteristics of the interference source on the power line are extracted when equipment runs normally. Then the finite difference time domain method is introduced to analyze the effects of the electromagnetic interference parameters on the security monitoring signal line. And the interference voltage of the two terminal sides on the single line is taken as evaluating indexes. Finally, the electromagnetic interference parameters are optimized by orthogonal experimental design based on the MATLAB simulation on the normal operation of equipment.

Keywords Security monitoring system · Finite difference time domain method (FDTD) · Electromagnetic interference (EMI) · Orthogonal experimental design

1 Introduction

With the development of coal mine automation, more and more high power electrical instruments have been used in coal mines. The underground electromagnetic interference has become particularly severe because the on-the-spot space is relatively narrow. At times EMI results in errors of the security monitoring system. Currently, there are hardly any research has been carried out in the field of coal mine EMC. Delogne (1991) generated a regulation of electromagnetic wave transmissions and indicated the difficulty of studying practical transmissions in tunnels. Hill (1989) studied the traveling wave in tunnels and radiation impedance of dipoles. Rappaport (1989) conducted a prediction using a ray tracing method. The references (Sun 1999; Sun et al. 2006) about the investigation into the wireless communication and channel studied the measurement for improving EMC system. These studies largely focused on wireless communication, which did not involve in the EMC studies in coal mines. Sun carried out a study of harsh classification on electromagnetic compatible measures of mining monitoring and communication equipment (Sun et al. 2008), as well as an investigation in coal mining EMC (Liang 2007; Zhang et al. 2007). References (Gao 2004; Liu et al. 2009, 2010) researched the region electromagnetic environment while the immunity of the monitoring was not involved. However, there has been no report about the effect of the electromagnetic interference parameters on the security monitoring system so far.

Security monitoring signal from sensors is often relatively weak, and its anti-interference ability is very poor in the process of transmission, which resulted in vulnerability to external electromagnetic interference. Therefore, it is very significant and important to reduce the interference voltage of security monitoring single line. In this paper, for the normal operation of equipment, the electromagnetic interference parameters of security monitoring signal line are optimized by using orthogonal experiment design

✉ Xiang Liu
13121434@bjtu.edu.cn; chqjiao@bjtu.edu.cn

[1] School of Electrical Engineering, Beijing Jiaotong University, Beijing 100044, China

method based on the finite difference time domain method (FDTD) analyses of multiple conductor transmission line (MTL) model, then the simulation experiments are carried out, and the electromagnetic interference voltage are decreased.

2 The basic electromagnetic interference theory of security monitoring system

2.1 Measurement and extraction of interference sources

The data of interferential voltage on device's power line while working normally can be obtained for many times by using the Amway 2711 spectrum analyzer. For all spectrum data measured, frequency-domain characteristic parameters are mainly analyzed, including the frequency band range of interference and the frequency distribution, etc. In order to investigate the average interference level on device's power line, the amplitude of each frequency point in the frequency domain is measured by using statistical analysis methods. Statistical analysis methods used are as follows: the interference data of the same type measured is analyzed; the average value at each frequency point is calculated; then connect all the points and draw the mean envelope. With analyzing all interference voltage spectrums on device's power line, the results of a statistical test are shown in Table 1. Figure 1 shows that the average value of envelope spectrum of interferential voltage on device's power line while working normally. With the increase of the frequency, the interferential voltage decreases rapidly when the frequency grows from 0.05 to 0.1 MHz; the interferential voltage increases briefly, then it decreases sharply when the frequency is between 0.1 and 0.2 MHz; the interferential voltage begins to flatten when the frequency is in the range of 0.1–0.7 MHz, and then to decline when the frequency is among 0.7–0.8 MHz; finally, when the frequency is higher than 0.8 MHz, the interferential voltage begins to flatten out again gradually, and it is the minimum value at this time.

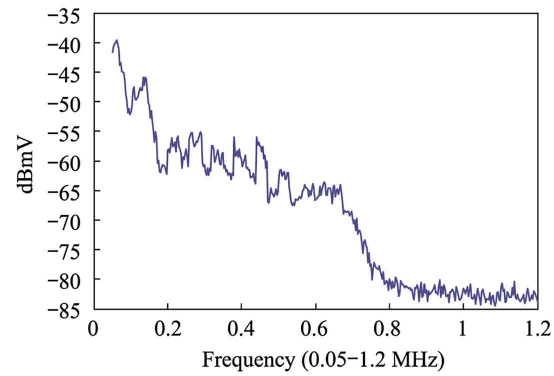

Fig. 1 The average value envelope spectrum of interferential voltage on device's power line while working normally

As shown in Fig. 1, the maximum interferential voltage value is 8.2327 V when the frequency is 0.05 MHz on device's power line while working normally. Therefore, interference sources can be taken as follows:

$$Vs = 8.2327 \times 10^{-6} \times \cos\left(2\pi \times 0.05 \times 10^{6} t\right)\ (\mathrm{V})$$

2.2 Numerical prediction model

The multi-conductor transmission line (MTL) structure can be described by the voltage and current iteration equations as follows (Erdin et al. 1998; Paul 2008; Jiao et al. 2012):

$$\frac{\partial V(z,t)}{\partial z} + L\frac{\partial I(z,t)}{\partial t} + RI(z,t) = V_F(z,t) \quad (1)$$

$$\frac{\partial I(z,t)}{\partial z} + C\frac{\partial V(z,t)}{\partial t} + GV(z,t) = I_F(z,t) \quad (2)$$

Table 1 The analysis of frequency-domain characteristic parameters of interference voltage on device's power line while working normally

No.	Frequency band range (MHz)	Frequency distribution (MHz)	0.05–0.4 MHz Mean voltage (dBmV)	0.4–0.8 MHz Mean voltage (dBmV)	0.8–1.2 MHz Mean voltage (dBmV)
1	0.05–0.806	0.067, 0.133, 0.283, 0.453	−53	−66	−83
2	0.05–0.773	0.053, 0.122, 0.378, 0.427	−54	−67	−83
3	0.05–0.788	0.064, 0.125, 0.228, 0.455	−59	−68	−82
4	0.05–0.785	0.056, 0.133, 0.263, 0.447	−55	−67	−83
5	0.05–0.78	0.062, 0.133, 0.26, 0.461	−55	−67	−82
6	0.05–0.772	0.064, 0.142, 0.292, 0.455	−55	−68	−83
7	0.05–0.76	0.053, 0.139, 0.378, 0.432	−55	−67	−83
8	0.05–0.766	0.064, 0.142, 0.323, 0.441	−56	−67	−83
9	0.05–0.749	0.062, 0.142, 0.28, 0.398	−54	−67	−83
10	0.05–0.743	0.073, 0.142, 0.22, 0.461	−55	−68	−83

where $V(z, t) = [V_1(Z, T), V_2(z, t),\ldots, V_n(z, t)]^T$ and $I(z, t) = [I_1(Z,T), I_2(z,t),\ldots, I_n(z,t)]^T$ represent the voltage and current vectors on the z point of line at moment t respectively; R, G, L, and C are resistive, inductive, conductive, and capacitive per-unit-length (p.u.l.) parameters of the line respectively; $V_F(z, t)$ and $I_F(z, t)$, respectively, denotes the excitation voltage source and motivation current source vectors on the z point at time t.

In this paper, the three-conductor transmission line is used as an example based on the coal mine security monitoring system, one of these is power line, the other two are signal lines as shown in Fig. 2. S-terminal and L-terminal represent two terminal sides of the transmission line. Infinite ground plane can be seen as reference, and the three lines are parallel.

There are two kinds of crosstalk of MTL: capacitive crosstalk and inductive crosstalk. The segment of the isometric lines is shown in Fig. 3, where V_S is the excitation source, V_1 and I_1 are the starting point of voltage and current, dz is the space step.

Because R and G in the lossless uniformed MTL are zero, the spatial discretization for MTL is along the transmission line based on the method of FDTD. The following results are obtained as Formula (3) and (4):

$$V_k^{n+1} = V_k^n - \frac{\Delta t}{\Delta z} C^{-1}\left(I_k^{n+1/2} - I_{k-1}^{n+1/2}\right) k = 2, 3, \ldots, NDZ \tag{3}$$

$$I_k^{n+3/2} = I_k^{n+1/2} - \frac{\Delta t}{\Delta z} L^{-1}\left(V_{k+1}^{n+1} - V_k^{n+1}\right) k = 1, 2, \ldots, NDZ \tag{4}$$

where subscript k denotes the spatial discretization sequence, superscript n is the time step point. Use 0 as the voltage superscript initial value, 1/2 as the current superscript initial value. We assume that the initial value of the voltage and current of transmission line is zero. It can be seen in the formula, the current on the conductor could be solved by iteration of the current moment voltage and

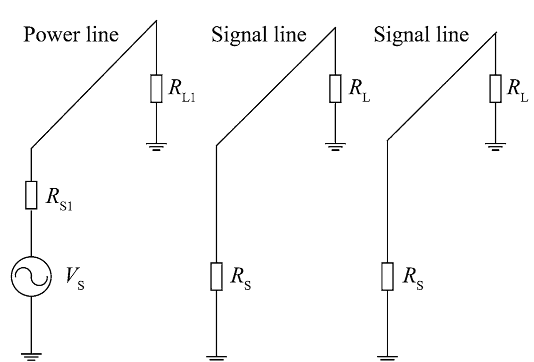

Fig. 2 Model of three parallel conductor transmission lines

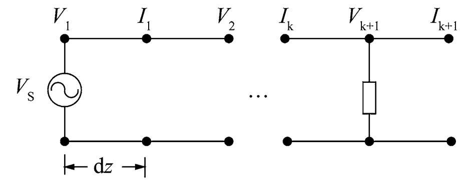

Fig. 3 Spatial discrete of parallel conductors

before a moment voltage. Otherwise the voltage can be solved by iteration of current.

Combine with the terminal conditions of the transmission line, we can get the difference equation of both S-terminal and L-terminal side as Formula (5) and (6):

$$\begin{aligned} V_1^{n+1} &= \left(R_S \frac{C}{2}\frac{\Delta z}{\Delta t} + \frac{E}{2}\right)^{-1} \times \left[\left(R_S \frac{C}{2}\frac{\Delta z}{\Delta t} - \frac{E}{2}\right)\right. \\ &\quad \left. \times V_1^n - R_S\left(I_1^{n+1/2} - I_0^{n+1/2}\right) + \frac{V_S^{n+1} + V_S^n}{2}\right] \\ &= \left(R_S \frac{C}{2}\frac{\Delta z}{\Delta t} + \frac{E}{2}\right)^{-1} \times \left[\left(R_S \frac{C}{2}\frac{\Delta z}{\Delta t} - \frac{E}{2}\right)\right. \\ &\quad \left. \times V_1^n - R_S I_1^{n+1/2} + \frac{V_S^{n+1} + V_S^n}{2}\right] \end{aligned} \tag{5}$$

$$\begin{aligned} V_{NDZ+1}^{n+1} &= \left(R_L \frac{C}{2}\frac{\Delta z}{\Delta t} + \frac{E}{2}\right)^{-1} \times \left[\left(R_L \frac{C}{2}\frac{\Delta z}{\Delta t} - \frac{E}{2}\right) V_{NDZ+1}^n\right. \\ &\quad \left. - R_L\left(I_{NDZ+1}^{n+1/2} - I_{NDZ}^{n+1/2}\right) + \frac{V_L^{n+1} + V_L^n}{2}\right] \\ &= \left(R_L \frac{C}{2}\frac{\Delta z}{\Delta t} + \frac{E}{2}\right)^{-1} \times \left[\left(R_L \frac{C}{2}\frac{\Delta z}{\Delta t} - \frac{E}{2}\right) V_{NDZ+1}^n\right. \\ &\quad \left. + R_L I_{NDZ}^{n+1/2} + \frac{V_L^{n+1} + V_L^n}{2}\right] \end{aligned} \tag{6}$$

The Formula (3), (4), (5) and (6) constitute the basic iterative formula of the FDTD method to analysis of MTL.

3 Electromagnetic interference parameters by using orthogonal experiment design

The electromagnetic interference parameters for security monitoring system in coal mines during devices' normal working are optimized by orthogonal experimental design methods based on the MATLAB simulation on the interference processes.

3.1 Orthogonal experimental design

Among all the interference parameters, length of transmission line (φ), distance between the power line and signal line (d_1), distance between two signal lines (d_2),

Table 2 Interference parameters with their ranges and values at four levels

Interference parameters	Range	Level 1	Level 2	Level 3	Level 4
Length of transmission line φ (m)	90–900	90	210	540	900
Distance between the power line and signal line d_1 (cm)	10–100	10	20	50	100
Distance between two signal lines d_2 (mm)	2–5	2	3	4	5
Distance between the transmission line and ground d_0 (cm)	10–100	10	20	50	100
Load of terminal side of the signal line R (Ω)	10–10000	10	100	1000	10000

Table 3 Orthogonal table and results

No.	Factor					Evaluation value	
	φ	d_1	d_2	d_0	R	Voltage of S-terminal (V)	Voltage of L-terminal (V)
1	1	1	1	1	1	6.27×10^{-9}	6.05×10^{-10}
2	1	2	2	2	2	3.99×10^{-8}	1.31×10^{-8}
3	1	3	3	3	3	1.39×10^{-7}	1.57×10^{-7}
4	1	4	4	4	4	5.71×10^{-7}	6.33×10^{-7}
5	2	1	2	3	4	3.22×10^{-6}	3.48×10^{-6}
6	2	2	1	4	3	7.81×10^{-7}	8.28×10^{-7}
7	2	3	4	1	2	1.14×10^{-8}	4.12×10^{-9}
8	2	4	3	2	1	9.42×10^{-10}	4.24×10^{-11}
9	3	1	3	4	2	6.25×10^{-7}	1.19×10^{-7}
10	3	2	4	3	1	4.57×10^{-8}	1.10×10^{-9}
11	3	3	1	2	4	4.86×10^{-7}	7.01×10^{-7}
12	3	4	2	1	3	3.07×10^{-8}	4.11×10^{-8}
13	4	1	4	2	3	3.13×10^{-6}	4.36×10^{-6}
14	4	2	3	1	4	8.38×10^{-7}	2.34×10^{-6}
15	4	3	2	4	1	6.03×10^{-8}	9.76×10^{-10}
16	4	4	1	3	2	1.70×10^{-7}	2.58×10^{-8}
K_{1i}	K_{11}	K_{11}	K_{13}	K_{14}	K_{15}		
K_{2i}	K_{21}	K_{22}	K_{23}	K_{24}	K_{25}		
K_{3i}	K_{31}	K_{32}	K_{33}	K_{34}	K_{35}		
K_{4i}	K_{41}	K_{42}	K_{43}	K_{44}	K_{45}		
R_i	R_1	R_2	R_3	R_4	R_5		

distance between the transmission line and ground (d_0), load of terminal side of the transmission line (R) are the five most important factors for security monitoring system in coal mines. And the interference results were evaluated by interference voltage on two terminal sides (S-terminal and L-terminal) of the transmission line. Finally, an orthogonal experiment of five factors was designed, and four-level orthogonal array $L_{16}(4^5)$ was employed; this array specifies 16 experimental runs and has 5 columns.

The selected interference parameters, along with their ranges and levels, are given in Table 2. Considering the structural characteristics of the underground power lines, the impedance of the S-terminal of the power line is set to 2 Ω and the impedance of the L-terminal of the power line is set to 100 MΩ. The detailed scheme of orthogonal experiment and the numerical simulation results of interference voltage on the two terminal sides of the transmission line at different levels are listed in Table 3.

In the Table 3, K_{ji} represents the experimental indicator when each parameter is at levels 1–4, R_i is the difference between the lowest value and the highest value for each parameter. The deference equation of R_i is:

$$R_i = \max\{K_{1i}, K_{2i}, K_{3i}, K_{4i}\} - \min\{K_{1i}, K_{2i}, K_{3i}, K_{4i}\} \quad (7)$$

According to the above analysis, the minimum interference voltage can be concluded.

Table 4 Interference voltage of S-terminal at different levels (unit: V)

Interference parameters	Length of transmission line	Distance between the power line and signal line	Distance between two signal lines	Distance between the transmission line and ground	Load of terminal side of the transmission line
Level 1	1.89×10^{-7}	8.62×10^{-7}	3.61×10^{-7}	2.22×10^{-7}	2.83×10^{-8}
Level 2	1.00×10^{-6}	4.26×10^{-7}	8.37×10^{-7}	9.15×10^{-7}	2.12×10^{-7}
Level 3	2.97×10^{-7}	1.74×10^{-7}	4.01×10^{-7}	8.93×10^{-7}	1.02×10^{-6}
Level 4	1.05×10^{-6}	1.93×10^{-7}	9.41×10^{-7}	5.09×10^{-7}	1.28×10^{-6}
Maximal difference	8.62×10^{-7}	1.57×10^{-6}	5.80×10^{-7}	6.94×10^{-7}	1.25×10^{-6}

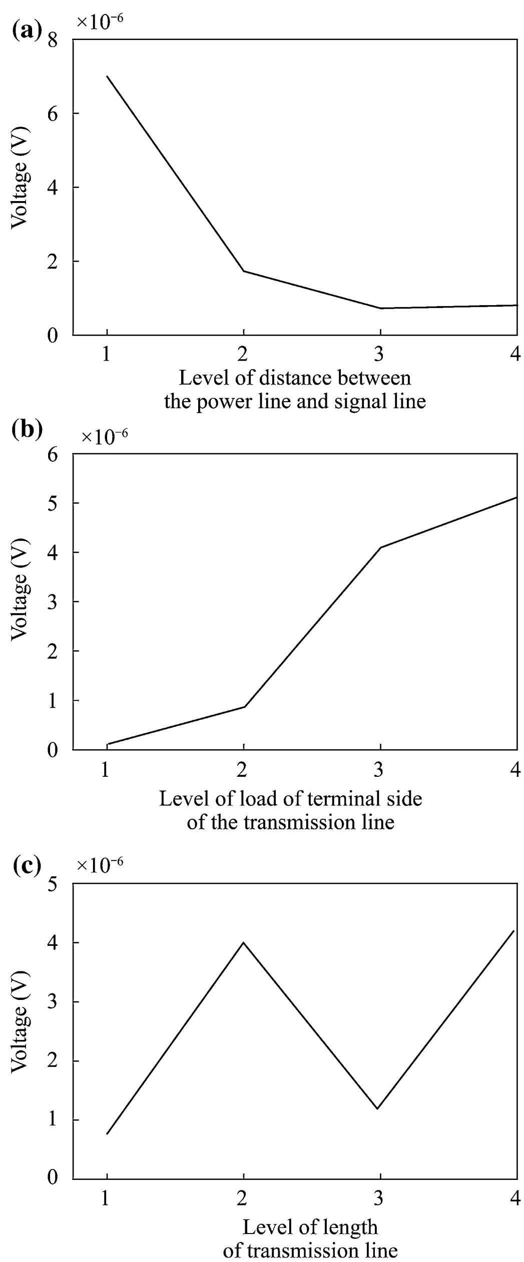

Fig. 4 Interference voltage of S-terminal for parameters at four levels. **a** Level of distance between the power line and signal line; **b** level of load of terminal side of the transmission line; **c** level of length of transmission line

3.2 Analysis of orthogonal experiment result

Considering the equipment to work normally, the interference voltage of S-terminal for each parameter at levels 1–4 and the difference between the lowest value and the highest value are listed in Table 4. By comparing the value of each parameter, it can be found that the three most significant parameters which influence the interference voltage of S-terminal are as follows: distance between the power line and signal line, load of terminal side of the transmission line and length of transmission line. The interference voltage of S-terminal for the three parameters at four levels is plotted in Fig. 4.

Figure 4a shows the variation of the interference voltage of S-terminal with the distance between the power line and signal line. With the increasing of distance between the power line and signal line, the interference voltage of S-terminal decreases at levels 1–4. Figure 4b shows the effect of the load of terminal side of the transmission line on the interference voltage of S-terminal. With the increasing of the load of terminal side of the transmission line, the interference voltage of S-terminal increases at levels 1–4. Figure 4c shows that the variation of the interference voltage of S-terminal with length of transmission line. It is observed that the length of transmission line at level 2 and level 3 are inflection points of the variation of the interference voltage of S-terminal, with the increasing of the length of transmission line; the interference voltage of S-terminal increases when the length of transmission line is lower than 100 Ω, then decreases when the length of transmission line is higher than 100 Ω and lower than 1000 Ω; finally, it increases when the length of transmission line is higher than 100 Ω.

Considering the equipment working in normal, the interference voltage of L-terminal for each parameter at levels 1–4 and the difference between the lowest value and the highest value are listed in Table 5. By comparing the value of each parameter, it can be found that the three most significant parameters which influences the interference voltage of L-terminal are as follows: the distance between the power line and signal line, load of terminal side of the transmission line and length of transmission line. The

Table 5 Interference voltage of L-terminal at different levels (unit: V)

Interference parameters	Length of transmission line	Distance between the power line and signal line	Distance between two signal lines	Distance between the transmission line and ground	Load of terminal side of the transmission line
Level 1	2.01×10^{-7}	1.99×10^{-6}	4.06×10^{-7}	5.97×10^{-7}	6.81×10^{-10}
Level 2	1.08×10^{-6}	7.96×10^{-7}	8.85×10^{-7}	1.29×10^{-6}	4.05×10^{-8}
Level 3	2.33×10^{-7}	2.33×10^{-7}	6.54×10^{-7}	9.17×10^{-7}	1.34×10^{-6}
Level 4	1.68×10^{-6}	1.75×10^{-7}	1.25×10^{-6}	6.95×10^{-7}	1.81×10^{-6}
Maximal difference	1.48×10^{-6}	1.82×10^{-6}	8.44×10^{-7}	3.20×10^{-7}	1.81×10^{-6}

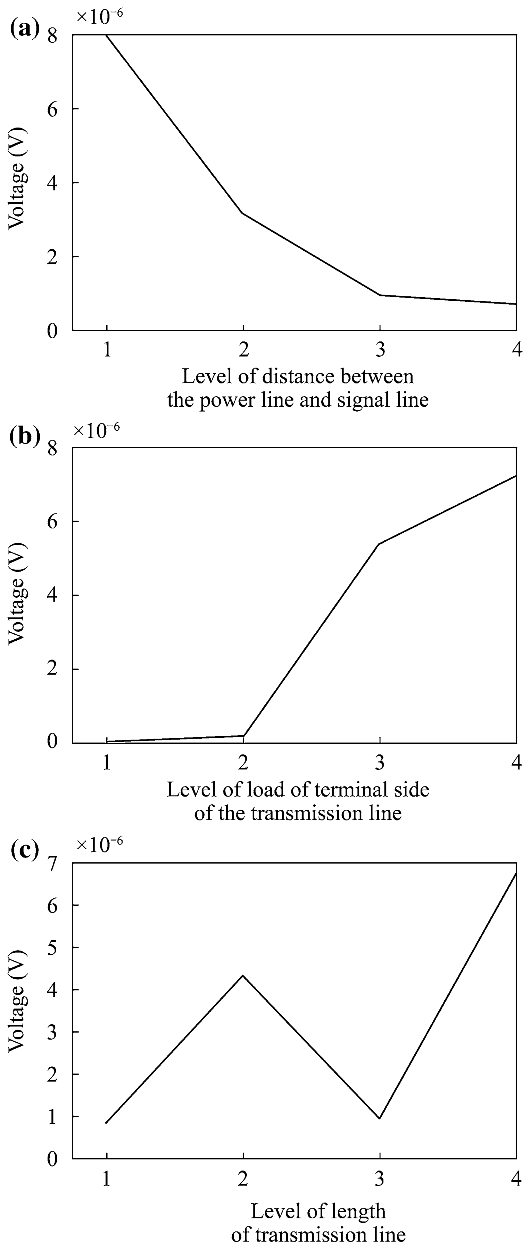

Fig. 5 Interference voltage of L-terminal for parameters at four levels. **a** level of distance between the power line and signal line; **b** level of load of terminal side of the transmission line; **c** level of length of transmission line

interference voltage of L-terminal for the three parameters at four levels is plotted in Fig. 5.

Figure 5 shows the variation of the interference voltage of L-terminal with the distance between the power line and signal line, the load of terminal side of the transmission line and the length of transmission line. It is observed that the variation of the interference voltage of L-terminal is similar to the variation of the interference voltage of S-terminal.

From Table 4 and Fig. 4, it is clear that the interference voltage of S-terminal is a minimal value at the third level of distance between the power line and signal line, at the

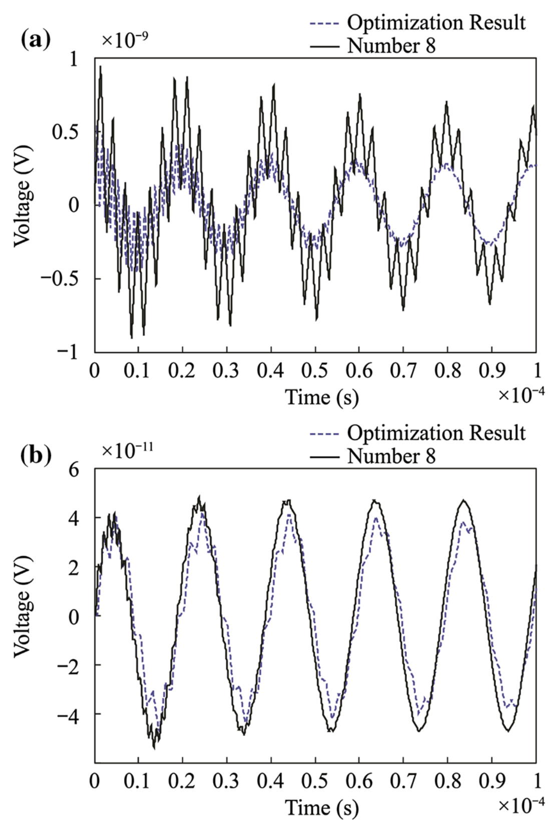

Fig. 6 Comparison-interference voltage of between optimization result and trial no. 8. **a** interference voltage of S-terminal; **b** interference voltage of L-terminal

Table 6 Comparison between the optimized and no. 8 simulation results

Interference voltage	The optimized simulation value (V)	simulation value of No. 8 (V)	Improvement effect (%)
Interference voltage of S-terminal	5.35×10^{-10}	9.42×10^{-10}	−43.21
Interference voltage of L-terminal	2.79×10^{-11}	4.24×10^{-11}	−34.20

first level of the load of terminal side of the transmission line, and at the first level of the length of transmission line. From Table 5 and Fig. 5, it is clear that the interference voltage of S-terminal is a minimal value at the forth level of distance between the power line and signal line, at the first level of the load of terminal side of the transmission line, and at the first level of the length of transmission line.

To sum up, the optimal parameters for the interference voltage of S-terminal and L-terminal are as follows: $\varphi = 90$ m, $d_1 = 50$ cm, $d_2 = 2$ mm, $d_0 = 10$ cm, $R = 10$ Ω.

4 Simulation experiment

From Table 3, it is observed that the minimal value of interference voltage of S-terminal and L-terminal among all the trials occur during the No.8 trial. To verify the optimization results of orthogonal experimental design, the comparison-interference voltage of S-terminal and L-terminal between the optimization result and No.8 trial as shown in Fig. 6.

Based on the orthogonal experimental design, the comparison between the optimized and No. 8 simulation results were performed and the results are listed in Table 6. As observed from the table, after the optimization, the interference voltage of the security supervision signal line was reduced at least 34.20 % before optimization.

5 Conclusions

In this paper, the frequency characteristics of interference source of the power line are extracted when equipment runs normally, the interference parameters are optimized by using orthogonal experiment design method based on the FDTD analyses of MTL on device's power line while working normally, and the results of experimental design are confirmed by MATLAB simulation. Conclusions are as follows:

(1) The interference source on device's the power line while working normally can be obtained by using the Amway 2711 spectrum analyzer; the optimal interference parameters obtained using orthogonal experiment design are as follows: length of transmission line is 90 m, distance between the power line and signal line is 50 cm, distance between two signal lines is 2 mm, distance between the transmission line and ground is 10 cm, load of signal line port is 10 Ω.

(2) Among the interference parameters, the distance between the power line and signal line is the most important one to affect the interference voltage of S-terminal and L-terminal; with the increase of the distance, the interference voltage of S-terminal and L-terminal decreases.

(3) The experiments on the electromagnetic interference of coal mine power system to security monitoring system show that electromagnetic interference can be decreased at least 34.20 %, which providing certain theoretical guidance for engineering practice.

Acknowledgments This study is supported by the Fundamental Research Funds for the Central Universities (No. 2014JBM116) and (No. 2014JBZ017).

References

Delogne P (1991) EM Propagation in tunnels. IEEE Trans Antennas Propag 39(3):401–405

Erdin I, Khazaka R, Nakhla M (1998) Simulation of high-speed interconnects in a multilayered medium in the presence of incident field. IEEE Trans on Microw Theory Tech 46(12):2251–2257

Gao YG (2004) Shielding and earthing. Beijing University of Posts and Telecommunications Press, Beijing, pp 61–65

Hill DA (1989) Reflection coefficient of a waveguide with slightly uneven walls. IEEE Trans Microw Theory Tech 37(1):244–252

Jiao CQ, Xia ZJ, Fu WN (2012) A generalized multiconductor transmission line model and optimized method for the solution of the MTL equations. Int J Antennas Propag 7

Liang ZG (2007) Theory, technique and application of electromagnetic compatibility. China Machine Press, Beijing, pp 35–37

Liu XQ, Wei GH, Pan XD (2009) Simulation and analysis of field performance in reverberation chamber with materials of different permeability. High Volt Eng 35(8):1986–1989

Liu XQ, Wei GH, Pan XD (2010) Numerical analysis on field performance optimization of reverberation chamber using dual-feeding. High Volt Eng 36(5):1234–1239

Paul CR (2008) Analysis of multiconductor transmission line. John Wiley & Sons, New York

Rappaport TS (1989) Characterization of UHF multipath radio channels in factory building. IEEE Trans Antenna Propag 37(8):1058–1069

Sun JP (1999) Harsh classification on electromagnetic compatible measure of mining monitoring and communication equipment. Coal Sci Technol 6:23–25

Sun JP, Pan T, Tian ZJ (2006) Study on electromagnetic compatibility in coal mining. J China Coal Soc 31(3):377–379

Sun JP, Ma FY, Li C (2008) Improved complex filter applied in enhancing EFT/B immunity at a coal mining monitoring substation. J China Univ Min Technol 18(1):22–26

Zhang SX, Xu ZH, Qian ZP (2007) Analysis of shielding effect of metallic box with apertures using FDTD. J PLA Univ Sci Technol (Nat Sci Edn) 8(4):324–327